



# The rheological behaviors, aging properties, and thermal stability of chain extended poly(butylene adipate-co-terephthalate)

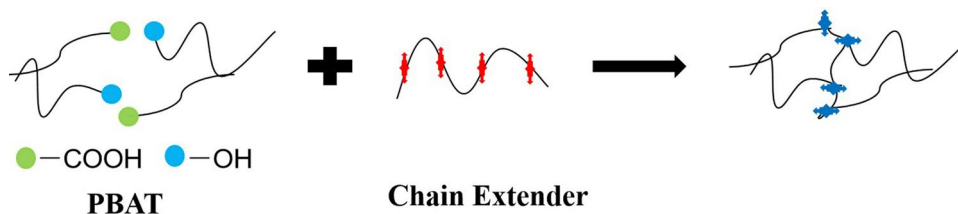
Yanping Hao<sup>1</sup> · Leilei Chen<sup>1</sup> · Fan Wang<sup>1</sup> · Qingkui Chen<sup>1</sup> · Shuangli Li<sup>1</sup> · Weiwei Zhang<sup>1</sup> · Shengnan Zhang<sup>1</sup> · Hongchi Tian<sup>1</sup> · Huili Yang<sup>2</sup>

Received: 15 March 2024 / Revised: 11 July 2024 / Accepted: 22 July 2024  
© Korean Society of Rheology 2024

## Abstract

In this work, a one-step reactive extrusion method was adopted to improve comprehensive properties of poly(butylene adipate-co-terephthalate) (PBAT) by melt blending with two chain extenders, including polycarbodiimide (PCDI) and multi-functional epoxy polymer (ADR). Their influences on rheological behaviors, aging properties, and thermal stability of PBAT were explored, and the detailed mechanisms were also discussed. It was found that the terminal carboxyl content of PBAT decreased with addition of PCDI and ADR. When 1.0 wt% PCDI was added, the terminal carboxyl content decreased by 70.3%. This indicated that the reaction between the two chain extenders and the terminal hydroxyl and carboxyl groups of PBAT enhanced to perform the chain extension, which increased the molecular weight, storage modulus, loss modulus, and complex viscosity of PBAT, and different relaxation processes were observed for different samples by Han and Cole–Cole plots. Damp-heat aging resistance measurements showed correlation with terminal carboxyl content in PBAT. And reducing the terminal carboxyl content in PBAT was shown to increase hydrolytic stability. For PBAT with 1.0 wt% PCDI blend, the tensile strength and elongation at break retention were above 70%. In addition, the thermal stability of PBAT was also improved due to the chain extension in the blends, which retarded degradation. The analysis results indicated that the comprehensive performance of modified PBAT was the best when 1.0 wt% PCDI was added.

## Graphical abstract



**Keywords** PBAT · Chain extension · Rheological behaviors · Aging properties · Thermal stability

## 1 Introduction

Nowadays, the most widely used films such as packaging film and mulching film are composed of low-density polyethylene (LDPE). However, PE films cannot be degraded after use, causing serious environmental pollution. Recently, researchers have focused on replacing the non-biodegradable products via the development of new biodegradable materials which can overcome the environmental pollution and landfill crisis [1]. One of the most promising and

✉ Yanping Hao  
13596069842@sina.cn

<sup>1</sup> Shandong Dawn Polymer Co., Ltd, Longkou 265700, China

<sup>2</sup> Key Laboratory of Polymer Ecomaterials, Chinese Academy of Sciences, Changchun Institute of Applied Chemistry, Changchun 130022, China

commercially available polymers that have attracted the interest of many researchers is poly(butylene adipate-co-terephthalate) (PBAT). PBAT synthesizes from adipic acid, 1,4-butanediol, and dimethyl terephthalate. It has high melt strength and flexibility, high elongation at break and good processability, which is considered to be one of the best materials to replace LDPE [2]. Thus, PBAT has been widely used in the production of biodegradable films in packaging and agriculture fields [3, 4]. However, the service life of PBAT is short due to its poor aging properties and thermal stability, which limits its more applications.

Generally, the intrinsic performances of PBAT are almost totally dependent on its structure [5]. Therefore, it is significantly important to control the molecular structure of PBAT and increase its molecular weight to improve its performance and further expand the range of potential applications. The increased PBAT molecular weight can increase mutual entanglement of its molecular chains and, thus, hinder the movement of the molecular chains, it needs more energy to activate the molecular chain motion, and thus improve its aging properties and thermal stability. To perform this function, chain extending modification usually is an efficient approach, which can quickly and effectively increase the molecular weight of PBAT [6].

Currently, several functional groups like epoxy [7–9], isocyanate [10–12], or peroxide [13–15] have been evaluated as potential chain extenders for polyester materials. Among them, epoxy groups containing multi-functional chain extenders have been widely used in polyester modification due to its wide source, low cost, low toxicity, easily reaction with both carboxyl and hydroxyl groups, and few by-products. Li et al. [16] used ADR-4468 as a chain extender to modify PLA by the melt chain expansion strategy. The results showed that ADR effectively improves the molecular structure and performance of PLA, provides more paths for the high-performance and functionalization of PLA, and gives an idea for biodegradable materials to replace some traditional petroleum-based plastics, thus promisingly broadening the application area of PLA materials, especially in environmental protection. de Souza et al. [8] use ADR-4370 as a chain extender to improve the properties of PBAT. It was found that PBAT-2%ADR shows higher tensile properties, probably due to the hydrogen bonds and interactions of  $\pi$ - $\pi$  nature between the materials; in this case, the ADR can act as a reinforcing agent.

In fact, terminal carboxyl groups play an important role in the process of thermal degradation of PBAT, especially in the initial process. Polycarbodiimide (PCDI) is a polymer or oligomer containing cumulative double bonds ( $-N=C=N-$ ) which can react with the terminal carboxyl groups of PBAT to form a stable urea structure. It has been used to improve toughness, solvent, thermal stability wear resistance of polyethylene terephthalate, polylactide,

poly(p-dioxanone), polyamides or polyurethanes [17–19]. However, no reports exist about PBAT modified by PCDI and its properties. So, PCDI is chosen as a chain extender for PBAT. We hope to obtain the modified PBAT with good aging properties and thermal stability. In this study, PCDI was melt blended with PBAT using a twin-screw extruder. The effects of PCDI on the terminal carboxyl content, molecular weight, rheological behaviors, aging properties, and thermal stability of PBAT were studied in comparison with that of ADR.

## 2 Experimental

### 2.1 Materials

PBAT with melt flow index of 3.65 g/10 min (at 190 °C, 2.16 kg) was bought from Shandong Dawn Degradation Materials Co., Ltd (Shandong, China). Polycarbodiimide (PCDI) and epoxy-based chain extenders (ADR) in white powder were bought from Shanghai Langyi function materials Co., LTD, China and BASF (Germany), respectively.

### 2.2 Sample preparation

Prior to processing, PBAT was dried at 70 °C for 12 h. Then the corresponding materials according to Table 1 were blended uniformly with a high-speed agitator. Afterward, they were melted and mixed in a twin-screw extruder (KY Solution Group, China) with an L/D of 36:1. The screw speed was set at 200 rpm, and the temperatures of heating zones from the hopper to the extrusion die were respectively set at: 100–110–130–145–150–155–155–160–160–160–160 °C. The specimens for tests were fabricated using an injection molding machine, YIZUMI A5S, under the injection pressure of 100 bars and processing temperature of 150–190 °C from the hopper to injection side. In this case, at least five standard specimens applied to tensile tests were fabricated for each sample.

**Table 1** The mixing compositions of all samples

| Samples | PBAT (wt%) | PCDI (wt%) | ADR (wt%) |
|---------|------------|------------|-----------|
| PBAT    | 100        | 0          | 0         |
| PCDI0.5 | 100        | 0.5        | 0         |
| PCDI1.0 | 100        | 1.0        | 0         |
| ADR0.5  | 100        | 0          | 0.5       |
| ADR1.0  | 100        | 0          | 1.0       |

### 3 Characterization

#### 3.1 FTIR spectra

Fourier transform infrared (FTIR) in attenuated total reflectance (ATR) mode (Thermo Nicolet) was adopted to analyze the chemical variation of PBAT-based blends before and after reactive extrusion, the wavenumber ranging between  $500\text{ cm}^{-1}$  and  $4000\text{ cm}^{-1}$ . After collection, the data were normalized to eliminate the error caused by the thickness differences of slice cutting from the standard tested specimens.

#### 3.2 Terminal carboxyl content

The terminal carboxyl content was analyzed via direct titration. The sample (2.0 g) was dissolved under heating in a mixed solution of phenol/chloroform at a ratio of 2/3 (50 mL) and titrated with a standard solution of KOH-ethanol (KOH concentration is 0.05 mol/L known solution) using bromophenol blue indicator. At the endpoint of the titration, the color of the solution changed from yellow to blue. For the correction of readings, the blank was also run. Each sample was measured in triplicate, the average was considered when the difference does not exceed 2 mol/t, the terminal carboxyl content of PBAT and its blends was calculated by Eq. (1):

$$X = \frac{(V - V_0) \times C \times 10^3}{m}, \quad (1)$$

where  $X$ ,  $V$ ,  $V_0$ ,  $C$ , and  $m$  are the terminal carboxyl content (mol/t), the volume of titrant used for sample (mL), the volume of titrant used for blank (mL), the concentration of KOH-ethanol standard titrant (mol/L), and sample weight, respectively.

#### 3.3 Gel permeation chromatography

The molecular weight parameters of all samples were measured by gel permeation chromatography (GPC) using a waters instrument (e2695 HPLC). GPC columns were eluted with THF at  $25\text{ }^\circ\text{C}$  at 1 mL/min according to DB22/T 2015–2014 standard.

#### 3.4 Rheology

Rheological behaviors of all samples were characterized on a desktop rheometer (MCR92, Q01DBSL Anton Paar, Germany) equipped with a circular heating area of 100 mm in diameter, and the temperature of this work was set at  $190\text{ }^\circ\text{C}$ . The strain amplitude was fixed to 1.25% to obtain reasonable

signal intensities even at elevated temperature or low angular frequency to avoid the nonlinear response. The angular frequency range used during testing was 0.1–100 rad/s. The multiple parameters including storage modulus, loss modulus, and complex viscosity were characterized, and the corresponding data were recorded and output by the RheoCompass™ software.

#### 3.5 Melt flow index

Melt flow index (MFI) is the melt flow rate index, expressed in grams, extruded isothermally in 10 min under constant load through a die of standard dimensions. Before testing, all samples were immersed in water separately and placed in a vacuum oven at  $70\text{ }^\circ\text{C}$ . After 24 h and 48 h, the samples were removed from the water and dried in a vacuum oven at  $70\text{ }^\circ\text{C}$  for 12 h. Then MFI of all samples were determined with mPXRZ-400B melt flow indexer (Changchun, China) equipped with a standard die. The die had a smooth straight bore with a diameter of  $2.0955 \pm 0.0051\text{ mm}$  and a length of  $8.000 \pm 0.025\text{ mm}$ . The measurements were performed according to ASTM D 1238-82. The investigated temperature was  $190\text{ }^\circ\text{C}$ .

#### 3.6 Tensile tests

Tensile tests for all samples were conducted on a Universal Tester (Zwick Roell, Z010) according to the standard ISO527 at room temperature, with a cross head speed of 50 mm/min. Before testing, all samples were subjected to 0, 5, 10, 15, and 20 days of damp-heat (DH) aging at  $70\text{ }^\circ\text{C}$  temperature and 70% relative humidity (RH). At least five runs for each sample were measured, and the results were averaged.

#### 3.7 Thermal stability

Thermal stability of all samples was measured by thermogravimetric analysis (TGA, Perkin-Elmer TGA-7, USA) using simultaneous thermal analysis instrument. All PBAT-based materials with weight of  $10 \pm 0.2\text{ mg}$  were heated from room temperature to  $600\text{ }^\circ\text{C}$  at  $10\text{ }^\circ\text{C}/\text{min}$  under nitrogen. In addition, neat PBAT, PCDI1.0, and ADR1.0 samples were also conducted at four different heating rates (5, 20, 30, and  $40\text{ }^\circ\text{C}/\text{min}$ ) from room temperature to  $600\text{ }^\circ\text{C}$ .

## 4 Results and discussion

### 4.1 FTIR spectra

FTIR analysis provides important evidence for the reaction because it is sensitive and effective for structural

characterization. The FTIR spectra of neat PBAT, neat PCDI, neat ADR, PCDI1.0, and ADR1.0 are presented in Fig. 1. With addition of 1.0 wt% PCDI, it could be observed that the characteristic absorption peak of carbodiimide group at  $2110\text{ cm}^{-1}$  disappears, which suggested that carbodiimide groups reacted with the terminal groups of PBAT. However, with addition of 1.0 wt% ADR, the spectra almost unchanged. With respect to the ADR chain extender, it was a co-polymer containing multi-functional epoxy groups, which could react with the terminal groups of PBAT [8], cross-linking to form molecular structures with branched chains, and the possible ring opening mode of epoxy groups and reaction procedure are also illustrated in Scheme 1. The terminal carboxyl content and molecular weight could also prove the reactions between PBAT and chain extenders.

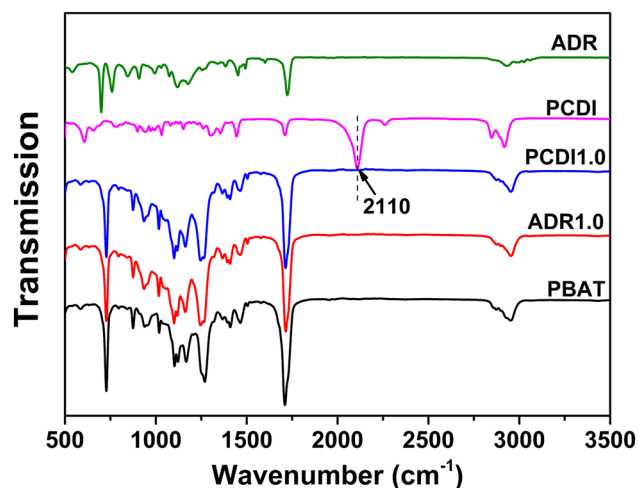


Fig. 1 FTIR spectra of neat PBAT, neat PCDI, neat ADR, PCDI1.0, and ADR1.0

## 4.2 Terminal carboxyl content and molecular weight

The terminal carboxyl content of PBAT is an important parameter for the indication of the chain extension reaction. Thus, the terminal carboxyl content of all samples was determined using the chemical titration method to prove that a chemical reaction occurred in modified PBAT. The terminal carboxyl content of all samples is shown in Fig. 2. It could be observed that modified PBAT showed lower terminal carboxyl content than that of neat PBAT due to the carbon–nitrogen double bond in PCDI, and the epoxy groups in ADR could react with the terminal carboxyl groups in PBAT to perform the chain extension, as shown in Scheme 1. In addition, for the same content of PCDI and ADR, PBAT/PCDI blends showed lower terminal carboxyl content than PBAT/ADR blends, suggesting that PCDI was more reactive with PBAT than ADR. In addition, the molecular weight of all samples was measured by

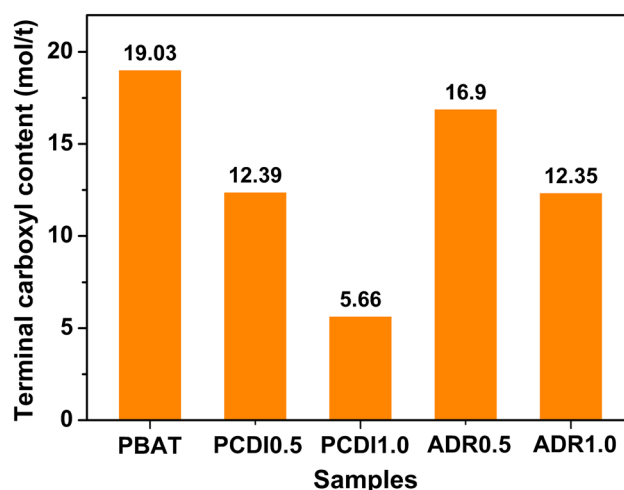
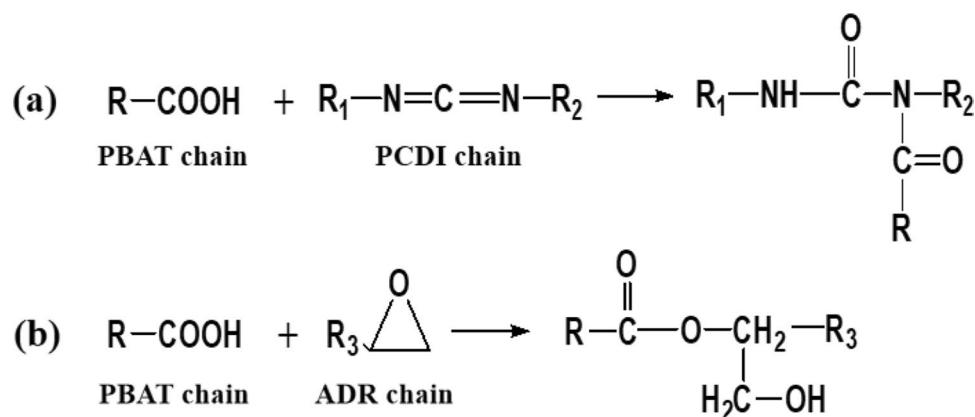


Fig. 2 Terminal carboxyl content of all samples

**Scheme 1** The reaction between **a** the carbon–nitrogen double bond of PCDI and **b** the epoxy group of ADR with the terminal carboxyl groups in PBAT



**Table 2** Molecular data of all samples

| Samples | $M_n$  | $M_w$  | PDI  |
|---------|--------|--------|------|
| PBAT    | 51,578 | 78,811 | 1.53 |
| PCDI0.5 | 53,494 | 82,916 | 1.55 |
| PCDI1.0 | 56,463 | 90,341 | 1.60 |
| ADR0.5  | 52,662 | 81,099 | 1.54 |
| ADR1.0  | 54,988 | 85,132 | 1.55 |

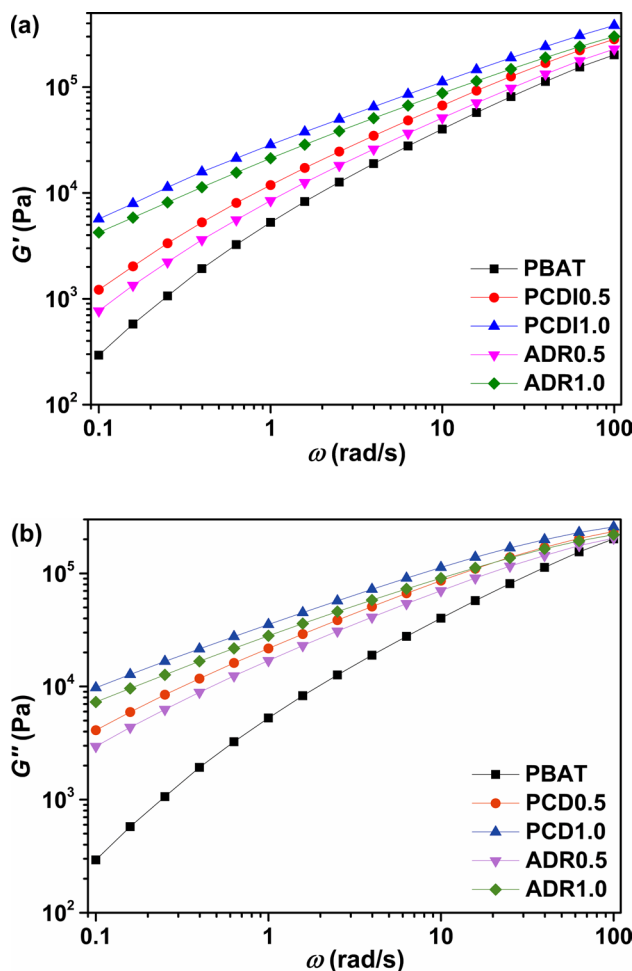
GPC, and the parameters are given in Table 2. As shown in Table 2, the molecular weight of modified PBAT was higher than that of neat PBAT, which also suggested that PBAT could react with both chain extenders to cause chain extension. The chain extension would widen the molecular weight distribution (PDI), which probably was the reason for the greater PDI of the modified PBAT than that of neat PBAT, as listed in Table 2.

### 4.3 Rheological behaviors

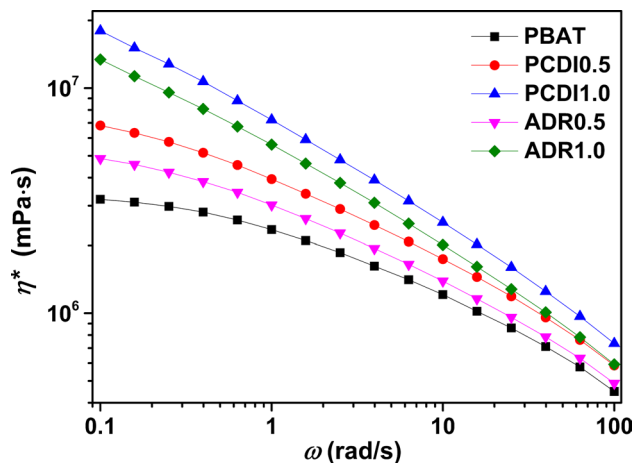
In general, there are two aspects of rheological measurements in the molten state. On the one hand, researching rheological performances can obtain the information of the processing ability [20]. On the other hand, the rheology is extremely sensitive to the molecular chain structure [21]. In this section, the rheological experiments were carried out for the samples.

Figure 3a, b shows the storage modulus ( $G'$ ) and loss modulus ( $G''$ ) as a function of angular frequency ( $\omega$ ) of all samples. It could be clearly observed that the  $G'$  and  $G''$  of modified PBAT gradually increased with increasing PCDI and ADR contents, especially at low angular frequency region. This might be because of the interaction between PBAT and the chain extenders, hindering the movement of molecular chain and making the relaxation of the molecular chain difficult, so the  $G'$  and  $G''$  were increased. On other hand, for the same content of PCDI and ADR, PBAT/PCDI blends showed higher  $G'$  and  $G''$  than PBAT/ADR blends, suggesting that the reaction activity of PCDI was higher than that of ADR.

Figure 4 shows the complex viscosity ( $\eta^*$ ) as a function of angular frequency ( $\omega$ ) of all samples. It could be seen that the  $\eta^*$  of all samples decreased with increasing angular frequency, which was the typical shear thinning behavior. After the addition of chain extenders, the magnitude of the  $\eta^*$  increased with increasing chain extender content, particularly at low angular frequency region. This correlated well with the increase in molecular weight with increasing chain extender content for the modified PBAT. For both chain extenders, at 1.0 wt% PCDI contents investigated, the  $\eta^*$  at  $\omega = 0.1$  rad/s was approximately one orders of magnitude



**Fig. 3** Plots of **a** storage modulus ( $G'$ ) and **b** loss modulus ( $G''$ ) versus angular frequency ( $\omega$ ) for all samples at 190 °C



**Fig. 4** Plots of complex viscosity ( $\eta^*$ ) versus angular frequency ( $\omega$ ) for all samples at 190 °C

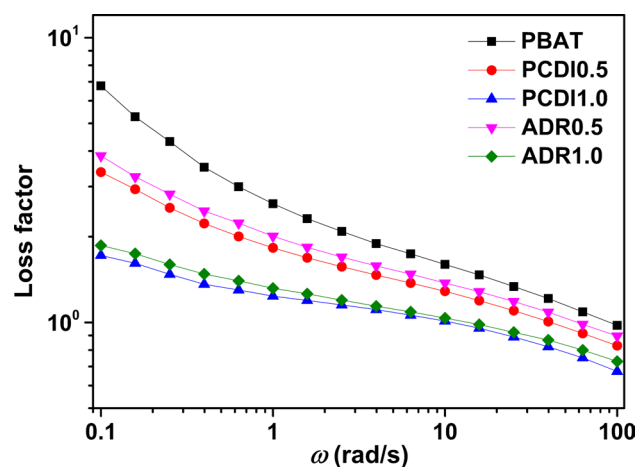


**Fig. 5** Plots of loss factor versus angular frequency ( $\omega$ ) for all samples at 190 °C

larger compared to the neat PBAT, and the shear thinning becomes more pronounced with chain extenders addition.

It was well known that the smaller the loss factor, the better the elasticity of the material. In Fig. 5, the modified PBAT presented smaller loss factors than that of neat PBAT, indicating the best elasticity of modified PBAT. It was reasonably convinced that the increasing elasticity was related to the extension of molecular chains. In addition, it was evident that the variation trend of loss factors was also in good agreement with that of GPC results (Table 2).

The Han curve can be used to study the structural differences between the neat polymer matrix and its blends. Figure 6a shows the Han plots of  $G'$  versus  $G''$  for all samples. Compared with neat PBAT, the Han curves of modified PBAT gradually moved upward and gradually approaches the diagonal. This might be because more chain extension reaction occurred in PBAT with high molecular weight, which strongly restricted the chain mobility of PBAT.

The strong restriction was further proved by the Cole–Cole plots shown in Fig. 6b, which was often adapted to the description of viscoelastic properties (viscosity and modulus) of the materials with a relaxation time distribution. As shown in Fig. 6b, the differences of neat PBAT and modified PBAT were very clear. For neat PBAT, the Cole–Cole plots were close to a semicircle. The curve of PCDI0.5 and ADR0.5 samples became level at high viscosity corresponding to low frequency. The Cole–Cole plots of PCDI1.0 and ADR1.0 samples were higher than that of the neat PLA, and showed more evident upturning at high viscosity, indicating that a longer relaxation time appeared. Through the above analysis, it was certain that a longer relaxation process appeared

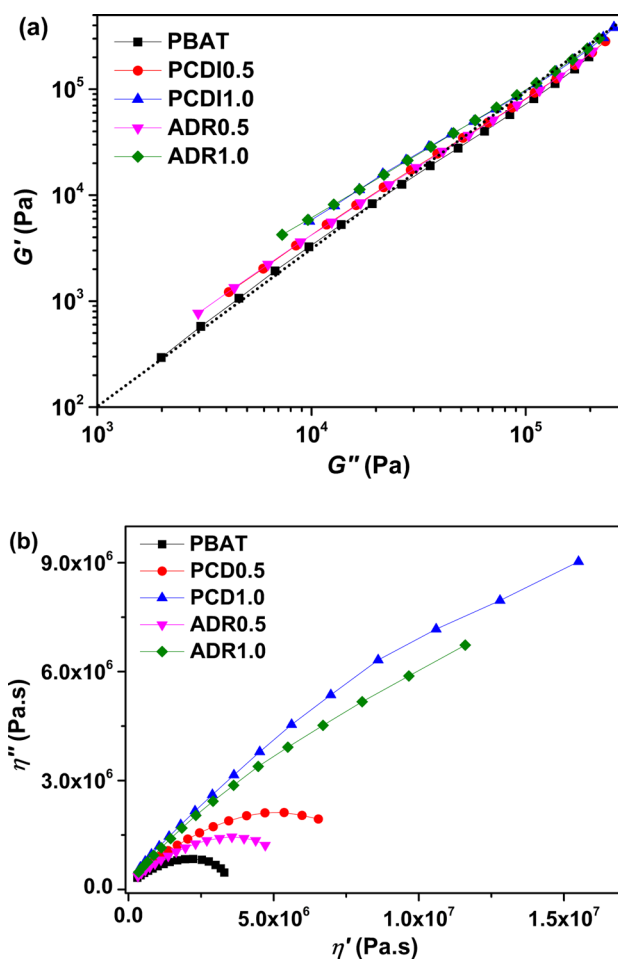


**Fig. 6** a Han and b Cole–Cole plots for all samples at 190 °C

in modified PBAT. It was also believed that this longer relaxation process was related to chain extension.

#### 4.4 Aging properties

Terminal carboxyl content has a certain effect on the aging properties of PBAT. In the previous analysis, we have used chain extenders to reduce the terminal carboxyl content of PBAT. In this part, we tested the changes of MFI before and after hydrolysis aging and the changes of mechanical properties before and after DH aging.

#### 4.5 Change of MFI before and after hydrolysis aging

Figure 7 displays the relationship between MFI and hydrolysis aging time. When chain extenders were introduced into PBAT, the MFI was reduced and the more chain extenders the samples contained, the lower their MFI was. This was because the chain extenders could react with PBAT chains (in Scheme 1) and the molecular chains became more intricate. Therefore, the melt flow became poorer. As seen in

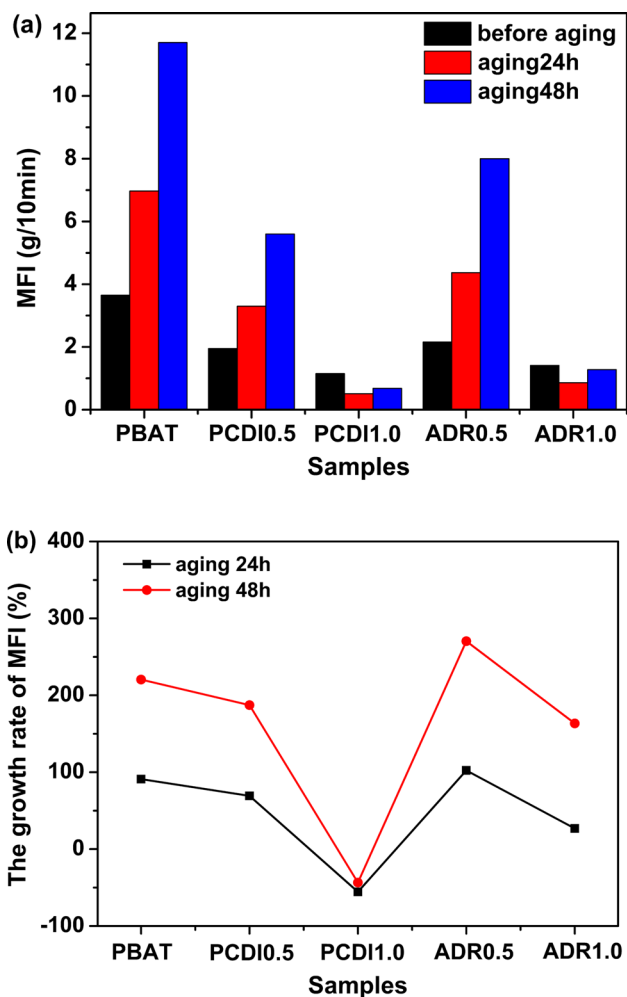


Fig. 7 Changes in **a** MFI and **b** the growth rate of MFI for all samples before and after aging

Fig. 7, the MFI of neat PBAT rapidly increased with increasing hydrolysis aging time. All modified PBAT showed the same variation trend in MFI, but their absolute MFI values were lower than that of neat PBAT and their variation was slower. This might be that the terminal carboxyl content of modified PBAT decreased after chain extension and the hydrolysis of carboxyl radical ( $-\text{COOH}$ ) was inhibited, improving the anti-aging properties of PBAT. Compared with PCDI and ADR, the MFI of PBAT with 1.0 wt% PCDI blend was the smallest because the reaction activity of PCDI was higher than that of ADR.

#### 4.6 Change of mechanical properties before and after DH aging

The effect of chain extenders on the mechanical properties of PBAT was investigated. Figure 8 presents the changes in the tensile strength and elongation at break of all samples with DH aging time. Before aging, it could be seen

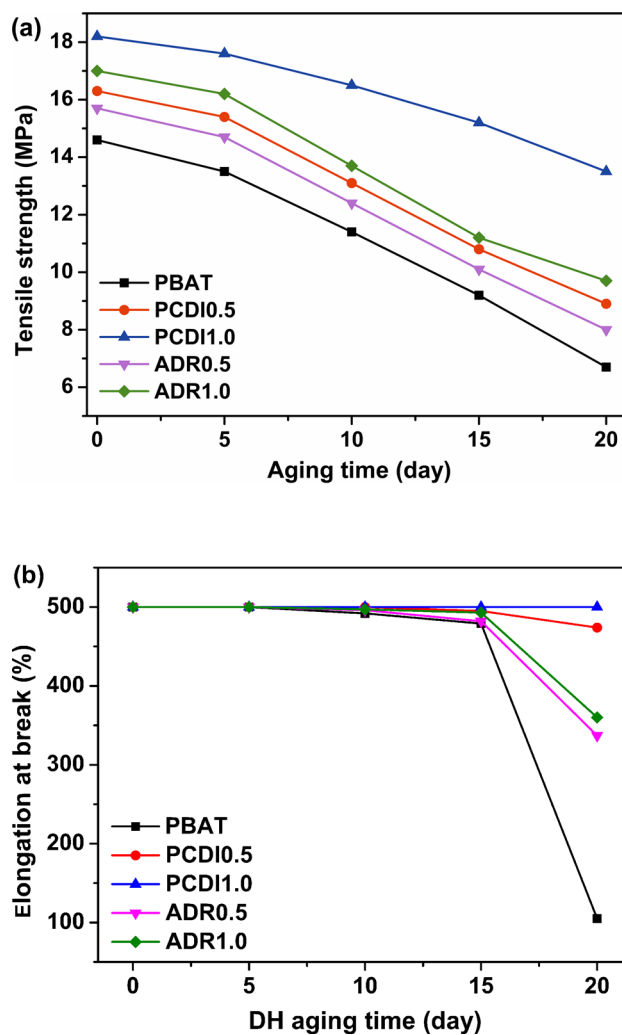


Fig. 8 Changes in **a** tensile strength and **b** elongation at break for all samples before and after aging

that the tensile strength of the samples gradually increased with the increasing content of chain extenders, and the elongation at break unchanged. The tensile strength of neat PBAT was 14.6 MPa and the elongation at break was 500%. When the addition of PCDI was 1.0 wt%, the tensile strength of modified PBAT was 18.2 MPa, which increased by 24.7% (3.6 MPa) compared with neat PBAT. Recently, some authors reported the reaction between polyesters and chain extenders, thereby increasing the tensile strength of polyesters [22–24]. Yang et al. investigated CDI-added PLA resins that displayed higher intrinsic viscosity and higher molecular weight, higher melt viscosity and lower melt flow index, higher tensile strength and longer elongation at break [18]. Chang et al. illustrated that the samples presented an enhancement in mechanical properties due to intermolecular forces after ADR addition [24]. Therefore, we inferred that the improvement in tensile strength was mainly because both chain extenders could react with PBAT to extend molecular

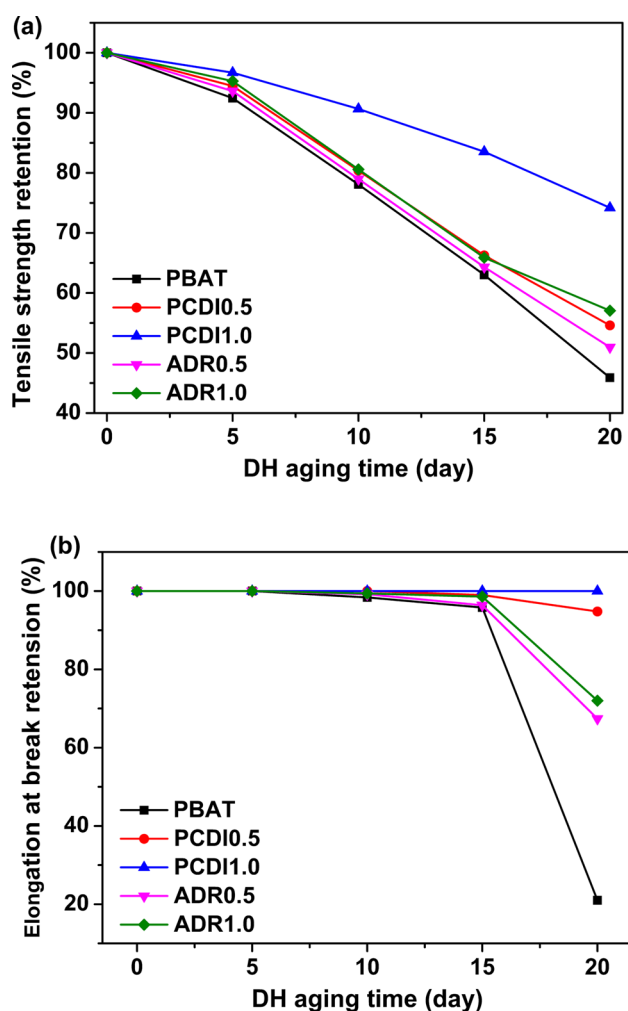


Fig. 9 Changes in **a** tensile strength retention and **b** elongation at break retention of all samples before and after aging

chain length and increase the molecular weight. At the same time, because PCDI was more reactive with PBAT than ADR, the molecular chain movement became more difficult, and the energy required for the molecular chain movement was increased, so it showed more excellent mechanical performances.

In addition, the tensile strength and elongation at break of all samples gradually decreased with increasing DH aging time, as shown in Fig. 8. Compared with neat PBAT, the tensile strength and elongation at break retention of modified PBAT increased significantly, as shown in Fig. 9. This was because the carbon–nitrogen double bond in PCDI and the epoxy groups in ADR could react with the terminal carboxyl groups in PBAT to perform the chain extension. At the same time, the hydrolysis of terminal carboxyl groups was inhibited, improving the anti-aging properties of PBAT.

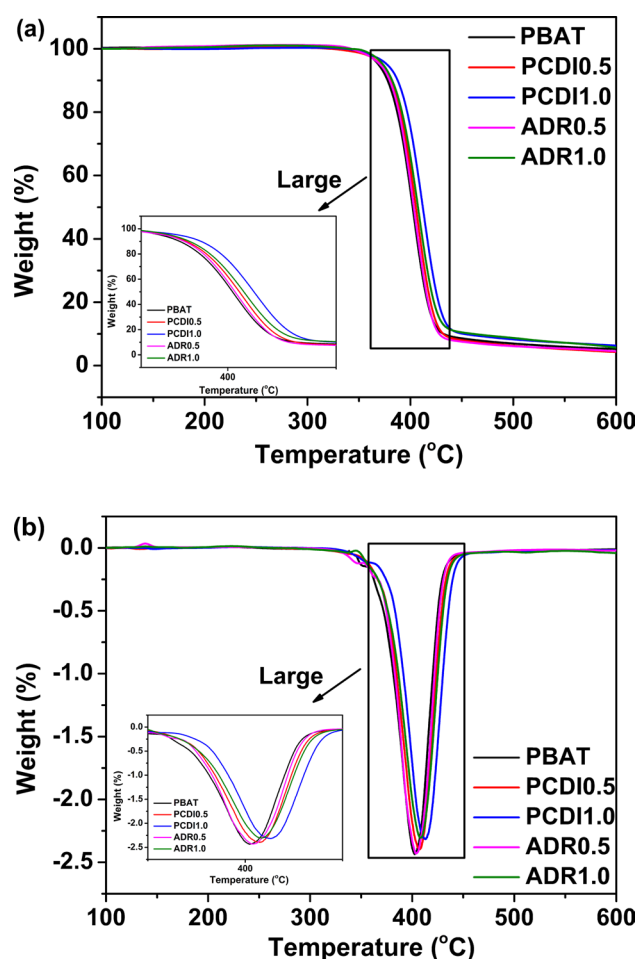


Fig. 10 **a** TGA and **b** DTG curves for all samples at a heating rate of 10 °C/min

## 4.7 Thermal stability

The integral (TGA) and derivative (DTG) thermogravimetric curves provide information about the nature and extent of degradation of the polymeric materials. The TGA and DTG traces for all samples in nitrogen atmosphere at a heating rate of 10 °C/min are shown in Fig. 10, and the corresponding parameters are given in Table 3. The thermal degradation behavior of various samples was compared using the initial decomposition temperature ( $T_{\text{onset}}$ ) and the temperature

Table 3 TGA data of all samples

| Samples | $T_{\text{onset}}$ | $T_{\text{max}}$ | $T_{0.2}$ | $T_{0.5}$ |
|---------|--------------------|------------------|-----------|-----------|
| PBAT    | 377.69             | 402.24           | 387.71    | 402.21    |
| PCDI0.5 | 380.91             | 407.34           | 390.08    | 405.34    |
| PCDI1.0 | 387.56             | 412.35           | 396.89    | 412.08    |
| ADR0.5  | 379.80             | 403.65           | 388.76    | 403.36    |
| ADR1.0  | 382.23             | 408.29           | 391.89    | 407.35    |



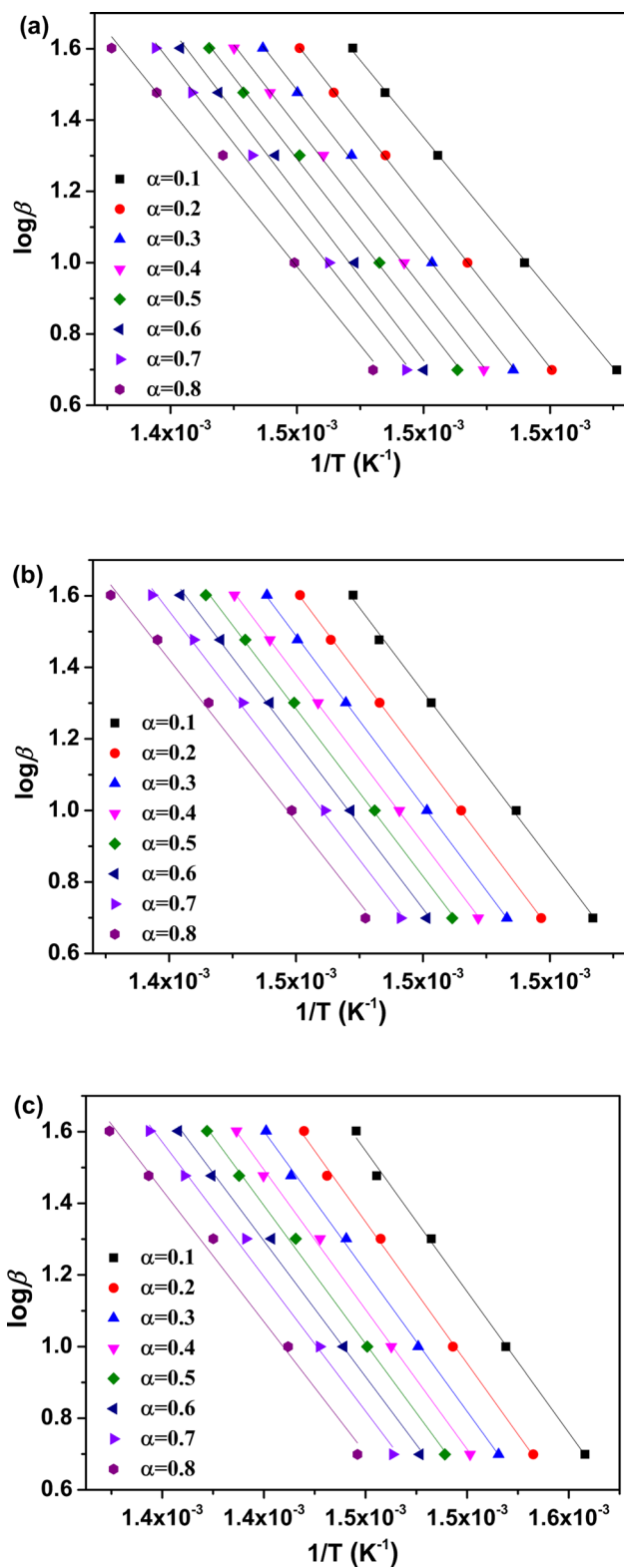


Fig. 11 Flynn–Wall–Ozawa plots at the following different weight losses of samples with different resolutions: **a** PBAT, **b** PCDI1.0, and **c** ADR1.0

of maximum rate of weight loss ( $T_{max}$ ) to understand the effects of chain extenders on the thermal degradation process of PBAT. Neat PBAT started to decompose at  $377.69\text{ }^{\circ}\text{C}$  ( $T_{onset}$ ). After that, the weight loss increased quickly, and the maximum degradation rate occurred at  $402.24\text{ }^{\circ}\text{C}$  ( $T_{max}$ ). As shown in Fig. 10a,b, the  $T_{onset}$  and  $T_{max}$  of modified PBAT slightly shifted to higher temperature, especially for PCDI1.0. Compared with neat PBAT, the  $T_{onset}$  and  $T_{max}$  of PCDI1.0 were increased by  $9.87$  and  $10.11\text{ }^{\circ}\text{C}$ , respectively, as shown in Table 3. In addition, the characteristic thermal degradation temperatures, including  $T_{0.2}$  and  $T_{0.5}$ , defined as the temperature at which 20% and 50% mass loss occurred, respectively, are also summarized in Table 3. It could be clearly observed that  $T_{0.2}$  and  $T_{0.5}$  increased with addition of chain extenders.

This improvement in the thermal stability could be attributed to the longer polymer chains produced in the modified PBAT, and hence the reduced number of chain ends per mass. Besides, PBAT/PCDI blends formed more longer polymer chains than that of PBAT/ADR blends, so PBAT/PCDI blends showed more excellent thermal stability.

The dynamic TGA method also is a promising tool to unravel the mechanisms of physical and chemical processes that occur during polymer degradation. Generally, for polymer degradation, all kinetic studies assume that the isothermal rate of conversion  $d\alpha/dt$  is proportional to the concentration of reacted material. The rate of conversion can be expressed by the following basic rate equation:

$$\frac{d\alpha}{dt} = k(T)f(\alpha), \tag{2}$$

where  $f(\alpha)$  and  $k(T)$  are function of conversion and temperature, respectively.

$k(T)$  is often modeled successfully by Arrhenius equation:

$$k(T) = A \exp\left(-\frac{E\alpha}{RT}\right), \tag{3}$$

where  $E_{\alpha}$  is the pyrolytic decomposition activation energy,  $A$  is the pre-exponential factor, and  $R$  is the gas constant.

$f(\alpha)$  depends on the particular decomposition mechanism. The simplest and most frequently used model for  $f(\alpha)$  in the analysis of TGA data is:

$$f(\alpha) = (1 - \alpha)^n, \tag{4}$$

where  $n$  is the order of reaction.

Insertion of Eqs. (3) and (4) into Eq. (2) gives

$$\frac{d\alpha}{dt} = \beta \frac{d\alpha}{dt} = A(1 - \alpha)^n e^{-\frac{E\alpha}{RT}}. \tag{5}$$

Flynn–Wall–Ozawa method [25] as per Eq. (5) is integrated using Doyle’s approximation [26], and the result of the integration after taking logarithms is:

**Table 4**  $r$  and  $E$  of samples by Flynn–Wall–Ozawa method

| Conversion( $\alpha$ ) | $r$       |           |           | $E$ (kJ/mol) |         |        |
|------------------------|-----------|-----------|-----------|--------------|---------|--------|
|                        | PBAT      | PCDI1.0   | ADR1.0    | PBAT         | PCDI1.0 | ADR1.0 |
| 0.1                    | − 0.99981 | − 0.99892 | − 0.99943 | 156.98       | 178.96  | 170.42 |
| 0.2                    | − 0.99995 | − 0.99920 | − 0.99994 | 164.84       | 179.96  | 171.89 |
| 0.3                    | − 0.99974 | − 0.99925 | − 0.99994 | 165.87       | 177.93  | 172.71 |
| 0.4                    | − 0.99966 | − 0.99917 | − 0.99993 | 166.40       | 177.55  | 171.14 |
| 0.5                    | − 0.99938 | − 0.99903 | − 0.99957 | 166.68       | 175.42  | 170.11 |
| 0.6                    | − 0.99782 | − 0.99843 | − 0.99937 | 169.69       | 172.42  | 170.11 |
| 0.7                    | − 0.99851 | − 0.99771 | − 0.99921 | 165.64       | 170.81  | 168.50 |
| 0.8                    | − 0.99572 | − 0.99585 | − 0.99801 | 160.22       | 167.15  | 164.87 |

$$\log F(\alpha) = \log \frac{AE\alpha}{R} - \log \beta - 2.315 - 0.4567 \frac{E\alpha}{RT}. \quad (6)$$

Thus, it is used to determine the activation energy for given values of conversion. The activation energy for different conversion values can be calculated from a  $\log \beta$  versus  $1/T$  plot.

The thermal degradation kinetic analysis of PBAT, PCDI1.0, and ADR1.0 was determined with Flynn–Wall–Ozawa method and the Flynn–Wall–Ozawa plots shown in Fig. 11. Figure 11 shows that the fitting lines were straight lines with a good correlation coefficient  $r$  as shown in Table 4, which indicated the applicability of Flynn–Wall–Ozawa to the systems in the conversion range investigated. The  $E_\alpha$  of PBAT, PCDI1.0, and ADR1.0 is also given in Table 4. Evidently, the  $E_\alpha$  of the modified PBAT was higher than those of neat PBAT at the same weight loss. It might be inferred that an increase in  $E_\alpha$  improved the thermal stability of PBAT.

## 5 Conclusion

In this study, two chain extenders, PCDI and ADR, were used to modify PBAT by reaction extrusion, and the effects of chain extenders on the rheological behaviors, aging properties, and thermal stability of PBAT were investigated in detail. First, a reduction in terminal carboxyl content, an increase in molecular weight, and a broadening of molecular weight distribution were found for both chain extenders, indicating that PBAT was successfully chain extended by the two chain extenders. Due to the reaction of chain extension, modified PBAT showed a remarkable improvement in storage modulus, loss modulus, and complex viscosity, especially at low angular frequency region, and different various relaxation mechanisms as well as longer relaxation time were revealed. Moreover, modified PBAT had better mechanical properties, aging performance, and thermal stability than that of neat PBAT. The

results also suggested that the comprehensive performance of modified PBAT with 1.0 wt% PCDI was excellent. Finally, this simple and convenient method of modification could balance the mechanical, aging, and degradation performances of PBAT, and it could be potentially applied in packaging.

**Acknowledgements** This work was supported by the fund of Yantai Science and Technology Innovation Development Plan (No. 2022ZDCX015) and Science and Technology Development Plan Project of Jilin Province China (No. 20240304161SF).

**Data availability** The authors confirm that the data supporting the findings of this study are available within the article [and/or its supplementary materials].

## Declarations

**Conflict of interest** The authors declare that we do not have any commercial or associative interest that represents a conflict of interest in connection with the work submitted.

## References

- Hao YP, Chen J, Liu Y, Wang F, Chen QK, Zhang WW, Zhang SN, Chen W, Tian HC (2023) Peroxide cross-linking and its role on the rheological, mechanical and thermal properties of poly(butylene adipate-co-butylene terephthalate). *Iran Polym J* 32:1271–1280
- Falcão GAM, Almeida TG, Bardi MAG, Carvalho LH, Canedo EL (2019) PBAT/organoclay composite films-part 2: effect of UV aging on permeability, mechanical properties and biodegradation. *Polym Bull* 76:291–301
- Rhim JW, Park HM, Há CS (2013) Bio-nanocomposites for food packaging applications. *Prog Polym Sci* 38:1629–1652
- Verdi AG, de Souza AG, Rocha DBM, de Oliveira SA, Alves RMV, dos Santos RD (2021) Biodegradable films functionalized with *Moringa oleifera* applied in food packaging. *Iran Polym J* 30:235–246
- Chang BZ, Li YC, Wang WS, Song G, Lin J, Murugadoss V, Naik N, Guo ZH (2021) Impacts of chain extenders on thermal property, degradation, and rheological performance of poly(butylene adipate-co-terephthalate). *J Mater Res* 36:3134–3144
- Tang D, Zhang CL, Weng YX (2021) Effect of multi-functional epoxy chain extender on the weathering resistance performance

- of poly(butylene adipate-*co*-terephthalate) (PBAT). *Polym Test* 99:107204(1–9)
7. Li B, Li J, Huang SW, Qin SH, Liu N (2023) Design of novel polylactide composite films with improved gas barrier and mechanical properties using epoxy chain extender-grafted organic montmorillonite. *J Polym Sci* 61:1572–1583
  8. De Souza AG, Nunes ECD, Rosa DS (2019) Understanding the effect of chain extender on poly(butylene adipate-*co*-terephthalate) structure. *Iran Polym J* 28:1035–1044
  9. Li Y, Wang L, Cheng HD, Han Y, Li DD (2024) Effect of carbon black and chain extender on thermal, rheological and mechanical properties of full biodegradable PBAT/P34HB blends. *Polym Inter*. <https://doi.org/10.1002/pi.6617>
  10. Song YH, Li J, Wang XR, Song GJ, Li XR, Cui YX, Feng ZY, Ning YK, Wu YM (2024) Grafting isocyanate onto graphene oxide for polyurethane composites to improve their thermal stability and mechanical properties. *Iran Polym J* 33:45–55
  11. Hao YP, Li Y, Liu ZG, Yan XY, Tong Y, Zhang HL (2019) Thermal mechanical and rheological properties of poly(lactic acid) chain extended with polyaryl polymethylene isocyanate. *Fiber Polym* 20:1766–2177
  12. Peng PW, Lee YH, Wang LY, Zhan YW, Chen ZY, Lee WF, Cheng YY (2024) Tuning the properties of bio-based thermoplastic polyurethane derived from polylactic acid by varying chain extenders and hard segment contents. *J Polym Environ*. <https://doi.org/10.1007/s10924-023-03183-4>
  13. Deetum C, Samthong C, Pratumpol P, Somwangthanaroj A (2017) Improvements in morphology, mechanical and thermal properties of films produced by reactive blending of poly(lactic acid)/natural rubber latex with dicumyl peroxide. *Iran Polym J* 26:615–628
  14. Signori F, Boggioni A, Righetti MC, Rondán CE, Bronco S, Ciardelli F (2015) Evidences of transesterification, chain branching and cross-linking in a biopolyester commercial blend upon reaction with dicumyl peroxide in the melt. *Macromol Mater Eng* 300:153–160
  15. Han CY, Ran XH, Su X, Zhang KY, Liu NA, Dong LS (2007) Effect of peroxide crosslinking on thermal and mechanical properties of poly( $\epsilon$ -caprolactone). *Polym Int* 56:593–600
  16. Li L, Wang HY, Jiang TJ, Hu C, Zhang JQ, Zheng HQ, Zeng GS (2023) Effect of epoxy chain extenders on molecular structure and properties of polylactic acid. *J Appl Polym Sci* 140:e54379(1–10)
  17. Hesselmans LCJ, Derksen AJ, Van den Goorbergh JAM (2006) Polycarbodiimide crosslinkers. *Prog Org Coat* 55:142–148
  18. Yang LX, Chen XS, Jing XB (2008) Stabilization of poly(lactic acid) by polycarbodiimide. *Polym Degrad Stabil* 93:1923–1929
  19. Ding SD, Liu ZP, Yang T, Zheng GC, Wang YZ (2010) Effect of polycarbodiimide on the thermal stability and crystallization of poly(p-dioxanone). *J Polym Res* 17:63–70
  20. Lyu Y, Chen YL, Lin ZW, Zhang JM, Shi XY (2020) Manipulating phase structure of biodegradable PLA/PBAT system: effects on dynamic rheological responses and 3D printing. *Compos Sci Technol* 200:108399(1–12)
  21. Li Y, Jia S, Du S (2018) Improved properties of recycled polypropylene by introducing the long chain branched structure through reactive extrusion. *Waste Manag* 76:172–179
  22. Li X, Xia M, Qiu D, Long R, Huang ZH, Li J, Long SJ, Li XF (2021) Fabrication and properties of modified poly(butylene terephthalate) with two-step chain extension. *Macromol Mater Eng* 306:2000638(1–12)
  23. Najafi N, Heuzey MC, Carreau PJ, Wood-Adams PM (2012) Control of thermal degradation of polylactide (PLA)-clay nanocomposites using chain extenders. *Polym Degrad Stabil* 97:554–565
  24. Chang BZ, Li YC, Wang WS, Song G, Lin J, Murugadoss V, Ni N, Guo ZH (2021) Impacts of chain extenders on thermal property, degradation, and rheological performance of poly(butylene adipate-*co*-terephthalate). *J Mater Res* 36:3134–3144
  25. Ozawa T (1965) A new method of analyzing thermogravimetric data. *Bull Chem Soc Jpn* 38:1881–1886
  26. Doyle CD (1961) Kinetic analysis of thermogravimetric data. *J Appl Polym Sci* 5:285–292

**Publisher's Note** Springer Nature remains neutral with regard to jurisdictional claims in published maps and institutional affiliations.

Springer Nature or its licensor (e.g. a society or other partner) holds exclusive rights to this article under a publishing agreement with the author(s) or other rightsholder(s); author self-archiving of the accepted manuscript version of this article is solely governed by the terms of such publishing agreement and applicable law.